

Protecting information in a parametrically driven hybrid quantum system

Siddharth Tiwary,^{1,2,*} Harsh Sharma,^{1,†} and Himadri Shekhar Dhar^{1,3,‡}

¹*Department of Physics, Indian Institute of Technology Bombay, Mumbai 400076, India*

²*Department of Physics, University of California, Berkeley, CA 94720, USA*

³*Centre of Excellence in Quantum Information, Computation, Science and Technology, Indian Institute of Technology Bombay, Mumbai 400076, India*

The transfer and storage of quantum information in a hybrid quantum system, consisting of an ensemble of atoms or spins interacting with a cavity, is adversely affected by the inhomogeneity of the spins, which negates the coherent exchange of excitations between the physical components. Using a full quantum treatment based on variational renormalization group, we show how quantum information encoded in the states of a parametrically driven hybrid system is strongly protected against any decoherence that may arise due to the inhomogeneity in the spin-ensemble.

I. INTRODUCTION

The development of quantum devices must often accommodate conflicting requirements, ranging from readily interacting qubits for information processing and communication to stable, protected states for storage of information [1]. An important cog in the contemporary quantum ecosystem that can overcome such conflicts is a hybrid system [2, 3], where the synergy between different physical systems is achieved by delegating tasks to components that offer specific advantages. For instance, while superconducting circuits are amenable for information processing [4], an ensemble of atoms or spins can offer longer coherence times for storage [5, 6]. Such ensembles can then be coupled to resonators that readily allow for transfer of information [7–10]. As such, hybrid systems based on spin-ensembles coupled to microwave cavities have gained significant traction in quantum information processing [8–13].

A key aspect of working with an ensemble of two-level atoms or spin-1/2 particles is that the transition frequencies for each particle may not be identical, a feature known as inhomogeneous broadening. Such broadening has the detrimental effect of decohering any information stored or transmitted from the ensemble to a coupled cavity, thus limiting the performance of any information processing protocol [14]. Over the years, several approaches have been proposed and implemented to overcome the effect of inhomogeneous broadening. A very natural recourse is the effect of “cavity protection”, whereby the coupling of the spin-ensemble with the cavity is significantly increased to suppress the decoherence arising due to the broadening [15–17]. Spin-ensemble based hybrid systems already offer the advantage of operating in the strong-coupling regime, due to the enhanced collective coupling strength of a large number of spins [8–10]. However, increasing this coupling further to suppress decoherence may require operational regimes, such as high-

Q cavities or increased spin density, which may either be difficult to implement or introduce unwanted spin interactions. Other approaches rely on refocusing mechanisms using spin-echo [18] or sophisticated engineering of the spectral distribution of the ensemble based on either optimal selection [19], dynamical decoupling [20] or hole-burning [21, 22]. While each method has its advantages, they often rely on complex control protocols or challenging experimental schemes to manipulate the spins, which may impede the performance of the hybrid system.

In this work, we propose a radically different method to overcome decoherence due to inhomogeneous broadening – one that does not involve altering the intrinsic spectral distribution of the spins but focuses on how information is encoded in the hybrid quantum system. In this approach, the quantum cavity is subjected to a parametric, two-photon drive, which exponentially enhances the coupling [23, 24] between the states of the cavity in the squeezed frame and the inhomogeneously broadened spin-ensemble. Therefore, any information now encoded in this new cavity frame experiences an implicit cavity protection effect. A clear advantage here is that by tuning the parametric driving strength, the effective coupling can be increased without resorting to the design of expensive cavities or the use of a high spin-density ensemble. Such enhancement in coupling has been studied in other contexts, including ultrastrong coupling between a few qubits and the cavity [25, 26], creation of entanglement [27, 28], superradiant phase transition [29, 30] and squeezed lasing [31].

To analyze the decoherence and subsequent cavity protection effect during the temporal evolution of the hybrid quantum system, we first look at the semiclassical equations of motion for the average photonic and spin excitations [32–34]. However, the study of protection of quantum information encoded in the photonic states requires a full quantum treatment, which is done using a variational renormalization method that captures the temporal dynamics of a driven-dissipative, spin-ensemble-cavity based hybrid system [35]. This then allows us to explicitly investigate any potential loss of information or fidelity of the encoded quantum state.

The paper is arranged in the following way. In Sec. II,

* siddharth110200@gmail.com

† harsh.sharma@iitb.ac.in

‡ himadri.dhar@iitb.ac.in

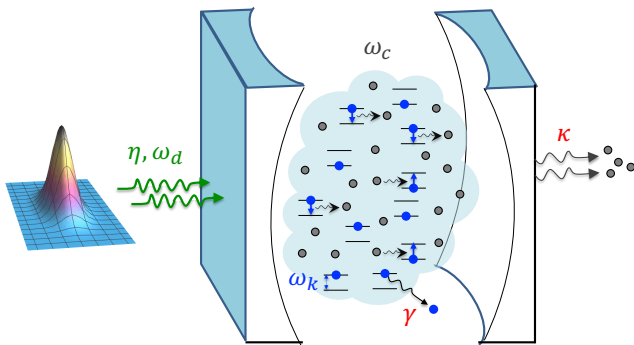


FIG. 1. A driven-dissipative hybrid quantum system, with N spins in an ensemble interacting with a cavity, with a frequency ω_c and driven by a parametric, two-photon drive with frequency ω_d and intensity η . The k^{th} spin in the ensemble has a transition frequency ω_k , and the spins and cavity lose excitations at rates γ and κ , respectively.

we look at the model that describes the dynamics of the hybrid system consisting of an ensemble of spins inside a cavity under parametric driving. In Sec. III, we derive the semiclassical equations for the photon and spin excitation operators and study the transition from weak to strong coupling regime. For full quantum solutions, we present the variational renormalization group method for driven-dissipative systems in Sec. IV, and show the protection effect under increasing driving strength. Finally, we end with a discussion of the main results in Sec. V.

II. THE EFFECTIVE HAMILTONIAN

The dynamics of a hybrid quantum system, consisting of an ensemble of N two-level atoms or spin-1/2 particles interacting with a quantum cavity, as shown in Fig. (1), is governed by the Tavis-Cummings model [36]. For a system subjected to a parametric, two-photon drive with a frequency ω_d , the corresponding Hamiltonian ($\hbar = 1$) under the rotating wave approximation (RWA) is given by,

$$\begin{aligned} \mathcal{H}_0 &= \frac{1}{2} \sum_{k=1}^N \Delta_k \sigma_k^z + \Delta_c \hat{a}^\dagger \hat{a} + \sum_{k=1}^N g_k (\sigma_k^- \hat{a}^\dagger + \sigma_k^+ \hat{a}) \\ &- \frac{\eta}{2} (\hat{a}^2 + \hat{a}^{\dagger 2}), \end{aligned} \quad (1)$$

where the system is in a frame rotating with half the driving frequency, $\omega_d/2$. The cavity and the spin transition frequencies are given by ω_c and ω_k for $k = 1, \dots, N$. The corresponding frequency detunings with respect to $\omega_d/2$ are $\Delta_{c,k} = \omega_{c,k} - \omega_d/2$. As usual, \hat{a} is the photon annihilation operator, $\{\sigma_k^z, \sigma_k^\pm\}$ are the spin operators given by the Pauli matrices, g_k is the coupling between the k^{th} spin and the cavity field, and η is the strength of the parametric drive.

For this study, the fundamental quantity of interest is the inhomogeneity of the spin ensemble, given by the

distribution of the spin transition frequencies ω_k and the spin-photon coupling g_k . The frequency distribution is taken to be Gaussian (cf. [37, 38]) with a standard deviation or width given by δ . For simplicity, the coupling is taken to be identical i.e., $g_k = g, \forall k$, which results in an effective coupling strength of $\Omega = \sqrt{\sum_{k=1}^N g_k^2} = \sqrt{N}g$. This demonstrates an enhancement of the coupling by a factor of \sqrt{N} compared to that of a single spin. Hence, ensembles with a high number of atoms or spins readily exhibit phenomena related to strong light-matter coupling even when individual particles couple only weakly to the cavity [9, 10].

Importantly, the effective spin-photon coupling can be further enhanced by parametrically driving the system. Using the unitary operator $\mathcal{U} = \exp[r(a^2 - a^{\dagger 2})/2]$, where $r = 1/2 \tanh^{-1}(\eta/\Delta_c)$ is the squeezing parameter, the cavity states can be transformed to a squeezed frame. The transformed spin-ensemble-cavity Hamiltonian is then given by $\mathcal{H}_{sq} = \mathcal{U}\mathcal{H}_0\mathcal{U}^\dagger$, such that

$$\begin{aligned} \mathcal{H}_{sq} &= \tilde{\Delta}_c \hat{a}_s^\dagger \hat{a}_s + \frac{1}{2} \sum_{k=1}^N \{ \Delta_k \sigma_k^z + g_k e^r (\hat{a}_s^- + \hat{a}_s^\dagger) (\sigma_k^- + \sigma_k^+) \\ &- g_k e^{-r} (\hat{a}_s - \hat{a}_s^\dagger) (\sigma_k^- - \sigma_k^+) \}, \end{aligned} \quad (2)$$

where $\tilde{\Delta}_c = \Delta_c / \cosh(2r)$ and $\hat{a}_s = \cosh(r)\hat{a} + \sinh(r)\hat{a}^\dagger$ is the cavity operator in the squeezed frame. For large r (i.e., $e^{-r} \rightarrow 0$), the Hamiltonian \mathcal{H}_{sq} is nothing but the inhomogeneous quantum Dicke model or the N -spin Rabi model in the squeezed frame, with an exponentially enhanced coupling $\tilde{g}_k = g_k e^r/2$. Moreover, \mathcal{H}_{sq} reduces to the Tavis-Cummings model in certain regimes where $|\tilde{\Delta}_c - \Delta_k| \ll \tilde{\Delta}_c + \Delta_k$ and $\tilde{g}_k \ll \tilde{\Delta}_c$, which ensures that RWA is valid for the transformed Hamiltonian and the system is not in the ultra-strong coupling regime [39, 40]. Therefore, the effective spin-cavity coupling in the transformed frame can be readily controlled simply by changing the parametric driving strength η .

Recently, such exponential enhancement in interaction strength was demonstrated in several experiments involving ion traps [41–43] and superconducting circuits [44]. In trapped-ion experiment [43], authors demonstrate amplification of interactions involving quantum harmonic oscillators, reaching squeezing as high as $r = 1.38$ with typical parameter values of $\omega_c/2\pi \sim 7$ MHz and $g/2\pi \sim 1.5$ KHz. For superconducting circuit experiment [44], a resonator is capacitively coupled to a transmon qubit and authors show two-fold increase in dispersive coupling corresponding to $r \approx 0.81$ for $\Delta_c/2\pi = 20$ MHz and $\eta/2\pi = 17$ MHz. Another experiment demonstrates detection of 15 dB squeezed vacuum states of light using degenerate parametric down conversion process. This corresponds to $r = 1.73$ and is the highest squeezing observed till now [45]. In all of these experiments, various decoherence processes (including squeezing induced decoherences) adversely affects the overall dynamics of the system and limits the maximum squeezing that can be achieved.

III. DYNAMICS IN THE SEMICLASSICAL REGIME

A key indicator to investigate the protection of information encoded in hybrid quantum systems is to investigate how quickly the average spin excitation or photon number in the cavity is lost as the system evolves. These quantities can be readily calculated using semiclassical equations of motion [32–34]. Now, in addition to inhomogeneity in the ensemble, the spins and the cavity in a hybrid system are also intrinsically lossy, i.e., they naturally lose coherence with time. Thus, the dynamics of a hybrid system is best described by a Lindblad master equation (ME), given by

$$\frac{d\rho}{dt} = -i[\mathcal{H}, \rho] + \kappa\mathcal{L}_{\hat{a}}[\rho] + \sum_k^n \{\gamma_h\mathcal{L}_{\sigma_k^-}[\rho] + \gamma_p\mathcal{L}_{\sigma_k^z}[\rho]\}, \quad (3)$$

where ρ is the density matrix of the system and the Lindblad operators are $\mathcal{L}_{\hat{x}}[\rho] = \hat{x}\rho\hat{x}^\dagger - \frac{1}{2}\{\hat{x}^\dagger\hat{x}, \rho\}$. The photon loss rate is κ , the rate of radiative decay and dephasing of spins is γ_h and γ_p . The equations of motion for the photonic and spin excitations, $\langle\hat{a}\rangle$, $\langle\sigma_k^-\rangle$ and $\langle\sigma_k^z\rangle$ are calculated using Eq. (3), for the Hamiltonian $\mathcal{H} = \mathcal{H}_0$. Using semi-classical (or mean-field) approximation in the limit of $N \rightarrow \infty$, all correlations between the emitters and the cavity can be ignored. This allows factorisation of all first-order correlations, i.e., $\langle\sigma_k^-\hat{a}\rangle \approx \langle\sigma_k^-\rangle\langle\hat{a}\rangle$, in the equations of motion of the hybrid system and we get,

$$\begin{aligned} \frac{d\langle\hat{a}\rangle}{dt} &= -(\kappa + i\Delta_c)\langle\hat{a}\rangle - i\sum_k g_k\langle\sigma_k^-\rangle + i\eta\langle\hat{a}\rangle^*, \\ \frac{d\langle\sigma_k^-\rangle}{dt} &= -(\gamma_h + 2\gamma_p + i\Delta_k)\langle\sigma_k^-\rangle + ig_k\langle\sigma_k^z\rangle\langle\hat{a}\rangle, \\ \frac{d\langle\sigma_k^z\rangle}{dt} &= -2\gamma_h(1 + \langle\sigma_k^z\rangle) + 2ig_k(\langle\sigma_k^-\rangle\langle\hat{a}\rangle^* - \langle\sigma_k^+\rangle\langle\hat{a}\rangle), \end{aligned} \quad (4)$$

where, $\langle a^\dagger \rangle = \langle a \rangle^*$ and $\langle \sigma_k^+ \rangle = \langle \sigma_k^- \rangle^*$. As the approximation ignores correlations between the ensemble and the cavity, it is not suited for studying quantum properties like entanglement and coherent exchange of information. However, it still allows the study of temporal evolution of average photon number and can even be used for large but finite N , away from criticality [33, 34].

By solving the equations above, we study the dynamics of a hybrid system consisting of an inhomogeneous ensemble of $N = 10^4$ spins. This ensemble is sufficiently large to use the semi-classical approximation in the stable region [34]. The key parameters used in the calculation are cavity detuning $\Delta_c = 70$ GHz, and the width of the spectral distribution, $\delta = 50 - 80$ MHz with mean $\Delta_k = \Delta_c$. The collective coupling is taken to be $\Omega = 40$ MHz and the parametric driving strength $\eta = \Delta_c \tanh(2r)$, with squeezing parameter $r = 0.0 - 2.4$. Also, to drive the system in linear regime, we ensure that $\tilde{g}_k \ll \tilde{\Delta}_c$. Moreover, to better characterize the effect

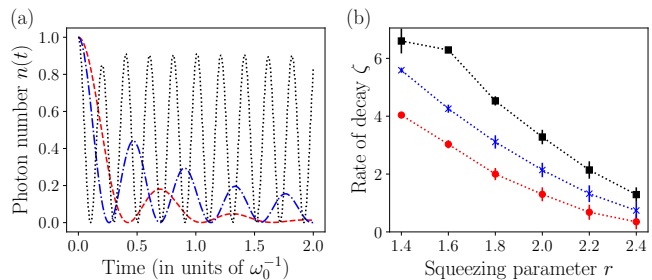


FIG. 2. Semiclassical dynamics of an ensemble of spins inside a cavity. The figures show (a) the time evolution of the average photon number $n(t) = |\langle\hat{a}\rangle_{sq}|^2$, for an ensemble with Gaussian frequency distribution of width $\delta = 60$ MHz and mean $\Delta_k = \Delta_c$, and squeezing parameter $r = 0.0$ (red dashed), $r = 1.0$ (blue dot-dashed), and $r = 2.0$ (black dotted), and (b) the variation in decay rate ζ with r , for width $\delta = 60$ MHz (red circle), $\delta = 70$ MHz (blue cross), and $\delta = 80$ MHz (black square). The error bars show the standard deviation between the actual value of $n(t)$ and those corresponding to the fitted decay rate ζ .

of inhomogeneous broadening in the semiclassical limit, the photon and spin losses are taken to be negligible as compared to the coupling and width of the distribution. These parameters typically corresponds to NV centres, but the dynamics is performed in the units of the cavity detuning and therefore as long as proper rescaling is ensured, it remains independent of absolute parameter values.

Figure 2 captures the dynamics of a hybrid system under parametric driving. The semiclassical equations are derived using the Hamiltonian \mathcal{H}_0 , such that the average photon number in the squeezed frame is given by $n(t) = |\langle\hat{a}_s\rangle|^2 = \cosh(2r)|\langle\hat{a}\rangle|^2 - \sinh(2r)\Re(\hat{a}^2)$, where r is the squeezing parameter. Similar results are obtained if one instead studies the equations of motion in the transformed frame by using \mathcal{H}_{sq} . In Fig. 2(a), the temporal evolution of $n(t)$ is shown for different values of squeezing parameter r , and a fixed width of the spin frequency distribution, $\delta = 60$ MHz. It is assumed that the hybrid system is initialized such that the cavity has photon number equal to unity i.e., $n(0) = 1$.

The figure shows that for $r = 0$, the average photon number quickly decoheres with time due to the inhomogeneity in the spin ensemble (other sources of dissipation have been ignored at this point). However, these excitations are sustained for higher values of r , which shows that boosting the parametric drive leads to a reduced decay rate and a longer lifetime for the photon. The rate at which the cavity excitation $n(t)$ is decohering can be captured by fitting the peaks of the Rabi oscillations using the relation, $n(t) = n(0)e^{-\zeta\omega_0 t}$, where ζ is a dimensionless quantity, and $\omega_0 = 10$ MHz is a reference frequency. So, higher ζ implies faster decoherence of the photonic excitations in the hybrid quantum system. Figure 2(b) shows the variation of the rate of decay ζ as a function of squeezing parameter r , for spin ensembles

of different width δ . The plots clearly show that loss of excitation and decoherence in the system is more severe for ensembles with more inhomogeneity (larger width δ). Importantly, parametric drives of increasing intensities, which give us higher values of r , are able to reduce the decay rate ζ successfully even for significantly broadened spin ensembles, thus giving an overall ‘‘cavity protection’’ effect. In fact, the protection is also observed when the inhomogeneity is larger than the effective coupling, i.e., $\delta > \Omega$, albeit in the absence of any other dissipation in the system.

In presence of cavity and qubit decoherences, following the calculations in Ref. [15] for $\kappa, \gamma_h, \gamma_p \ll \tilde{\Omega}$, it can be shown that the average photon number in the cavity decays at the rate, $\Gamma_n(\tilde{\Omega}) = \kappa + \gamma_h + 2\gamma_p + \pi\rho(\tilde{\Omega})\tilde{\Omega}^2$, where for Gaussian distribution of emitters, $\rho(\tilde{\Omega}) \sim 2^{-\tilde{\Omega}^2/\delta^2}/\delta$ governs the decoherence induced by inhomogeneous broadening and $\tilde{\Omega} = \Omega \cosh(r)$ is the effective coupling strength in the squeezed frame. For $\tilde{\Omega} \ll \delta$, due to Purcell effect, the decay rate increases on increasing r [16]. However, in strong coupling regime when $\tilde{\Omega} \gg \delta$, there is a protective energy gap between the superradiant and the subradiant spin-wave modes, which does not allow inhomogeneity to induce decoherence in the system [14]. As a result, an exponential decay in the decay rate Γ_n is observed and eventually the dynamics of the system becomes independent of inhomogeneous broadening. To quantify the suppression in errors due to inhomogeneity, we define the ratio,

$$\xi_r \equiv \frac{\Gamma_n(\tilde{\Omega})}{\Gamma_n(\infty)} - 1 = \frac{\pi\rho(\tilde{\Omega})\tilde{\Omega}^2}{\kappa + \gamma_h + 2\gamma_p}, \quad (5)$$

which becomes zero in the limit of $r \rightarrow \infty$.

IV. PROTECTING INFORMATION IN THE HYBRID SYSTEM

While semiclassical equations highlight the revival of macroscopic quantities such as the average photon number in the cavity, to study protection of information encoded in any superposed quantum state, the dynamics of the full quantum system is necessary. This is a computationally challenging task due to the large Hilbert space of the spin-ensemble-cavity system. To overcome this, we use a variational renormalization group method to study driven-dissipative dynamics [35], which is a tensor-network method similar to density matrix renormalization group and matrix-product states [46]. The method employs a time-adaptive approach to temporally evolve the density matrix ρ of a spin-cavity system of about hundred spins, using the Lindblad ME formalism. To achieve this, all states ρ and operators \hat{O} are mapped to a higher dimensional space as superkets $|\rho\rangle$ and superoperators \hat{O} i.e., $\rho \rightarrow \mathbf{vec}(\rho) = |\rho\rangle$ and $\hat{O}\rho \rightarrow (\hat{O} \otimes \mathbb{I})|\rho\rangle = \hat{O}|\rho\rangle$. This allows the master equation in Eq. (3) to be mapped to a Schrödinger like equation, $d|\rho\rangle/dt = \tilde{\mathcal{L}}|\rho\rangle$, in the

superoperator space, where

$$\tilde{\mathcal{L}} = -i(\mathcal{H} \otimes \mathbf{I} - \mathbf{I} \otimes \mathcal{H}^T) + \kappa \tilde{\mathcal{L}}_{\hat{a}} + \sum_k \{\gamma_h \tilde{\mathcal{L}}_{\sigma_k^-} + \gamma_p \tilde{\mathcal{L}}_{\sigma_k^z}\}, \quad (6)$$

and $\tilde{\mathcal{L}}_{\hat{x}} = \hat{x} \otimes \hat{x}^* - \frac{1}{2} \hat{x}^\dagger \hat{x} \otimes \mathbf{I} - \frac{1}{2} \mathbf{I} \otimes \hat{x}^T \hat{x}$. At this point, the variational renormalization has two key parts. First, finding the renormalized representation for the superket $|\rho\rangle$ in a significantly reduced subspace, and second, evolving the initial state $|\rho\rangle$ in a time-adaptive manner. As with most tensor-network methods, the renormalized space is obtained by eliminating the null space or those with marginal singular values. The time evolution is then governed using the Lindblad ME in Eq. (6), using the transformed Hamiltonian $\mathcal{H} = \mathcal{H}_{sq}$, and evolved adaptively for small intervals Δt , such that $|\rho(t + \delta t)\rangle = e^{\tilde{\mathcal{L}}\Delta t} |\rho(t)\rangle$. Now, $\tilde{\mathcal{L}} = \sum_k \tilde{\mathcal{L}}_k$, and the second-order Suzuki-Trotter decomposition helps expand $e^{\tilde{\mathcal{L}}2\Delta t}$ into a product of single spin-cavity evolution: $e^{\tilde{\mathcal{L}}_N \Delta t} e^{\tilde{\mathcal{L}}_{N-1} \Delta t} \dots e^{\tilde{\mathcal{L}}_1 2\Delta t} \dots e^{\tilde{\mathcal{L}}_{N-1} \Delta t} e^{\tilde{\mathcal{L}}_N \Delta t}$ (see Refs. [35, 47]). The computation then follows an iterative sweeping protocol as used in other time-adaptive tensor-network methods [48, 49].

We note that squeezing the cavity also transforms the Lindblad operator $\mathcal{L}_{\hat{a}}$, which is given by [25],

$$\begin{aligned} \mathcal{L}_{\hat{a}}[\rho] \rightarrow (n_{\text{th}} + 1)\mathcal{L}_{\hat{a}_s}[\rho] + n_{\text{th}}\mathcal{L}_{\hat{a}_s^\dagger}[\rho] \\ - m_{2\text{-ph}}\mathcal{L}'_{\hat{a}_s}[\rho] - m_{2\text{-ph}}^*\mathcal{L}'_{\hat{a}_s^\dagger}[\rho], \end{aligned} \quad (7)$$

where $\mathcal{L}'_{\hat{x}}[\rho] = \hat{x}\rho\hat{x} - \frac{1}{2}\{\hat{x}^2, \rho\}$ and $n_{\text{th}}, m_{2\text{-ph}}$ are functions of squeezing parameter r , which correspond to thermal noise and two-photon correlations introduced by squeezing, respectively. This effectively induces additional errors in the system, but these can be eliminated by coupling the cavity mode to a squeezed-vacuum reservoir with the same squeezing r , which is phase-shifted by π relative to the two-photon drive.

For the full quantum dynamics of the hybrid system using variational renormalization group, we consider an ensemble of $N = 100$ spins inside the cavity. For consistency with semiclassical results, we use the same set of parameters, including the collective coupling strength $\Omega = 40$ MHz. However, we now consider other dissipative terms, such as the photon loss rate $\kappa = 7$ MHz, and radiative loss and dephasing for spins equal to $\gamma_h = \kappa/8$ and $\gamma_p = \kappa/16$, respectively.

At the start, the quantum information is encoded in the effective state of the cavity in the squeezed frame, which at time $t = 0$ is given by $|\psi_c(0)\rangle$. As the dynamics is governed by the Lindblad ME, the cavity state at time t is given by the density matrix $\rho_c(t)$. To study the effect of decoherence and protection of information, we look at two distinct figures of merit, viz. quantum fidelity and the Wigner function. The quantum fidelity $\mathcal{F}(t)$ is taken between the state $\rho_c(t)$ at t and the initial state encoded in the system $|\psi_c(0)\rangle$, i.e., $\mathcal{F}(t) = \sqrt{\langle \psi_c(0) | \rho_c(t) | \psi_c(0) \rangle}$. The Wigner function allows us to study the phase-space properties of the encoded information, which is not captured by the fidelity,

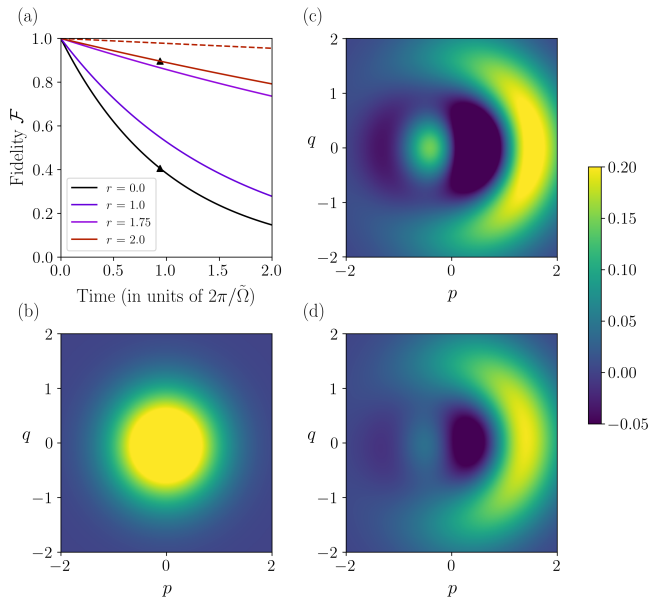


FIG. 3. Dynamics of quantum information encoded in a hybrid system consisting of $N = 100$ spins inside a cavity. The width of the frequency distribution is $\delta = 30$ MHz. The plots in (a) show the evolution of the fidelity \mathcal{F} between the effective cavity state at time t and the initial state at $t = 0$, for different r . The plot is the best-fit curve that envelops the fidelity. The dashed curve corresponds to the fidelity averaged over 100 Haar random initial states for $r = 2.0$. The other subfigures show the Wigner function $W(p, q)$ of the initial cavity state in (b), and the state at t corresponding to fidelity (black triangles in (a)) for parameters (c) $r = 0.0$ and (d) $r = 2.0$.

and is defined as $W(p, q) = \frac{1}{\pi} \int e^{2iqy} dy \langle p-y | \rho_c(t) | p+y \rangle$. It maps the density matrix in Hilbert space to a distribution in phase space but it still contains full information present in the quantum state. As such, when the dynamics is dominated by decoherences, any change in the Wigner function from its initial form indicates loss of information.

Figure 3 shows the fidelity of the information encoded in the initial state and the temporally evolving photon density matrix $\rho_c(t)$, as well as its quasi-probability distribution in terms of $W(p, q)$. Since our motive is to observe decoherence, we start with the maximally coherent initial cavity state $|\psi_c(0)\rangle = \frac{1}{\sqrt{2}}\{|1\rangle + |2\rangle\}$, where $|1\rangle$ and $|2\rangle$ are the Fock states in the transformed basis. This is because decoherence effect is the strongest when acting on the maximally coherent state as, loss terms leading to de-excitation such as κ and γ_h are more (less) effective on states with higher (lower) excitation, and the average loss of fidelity is close to that observed for an equal superposition or maximally coherent state. Moreover, effects of loss due to dephasing such as γ_p is most effective on maximally coherent states. In Fig. 3(a), the plot shows the best-fit envelope of the fidelity of the density matrix at t with the initially prepared superposition state that

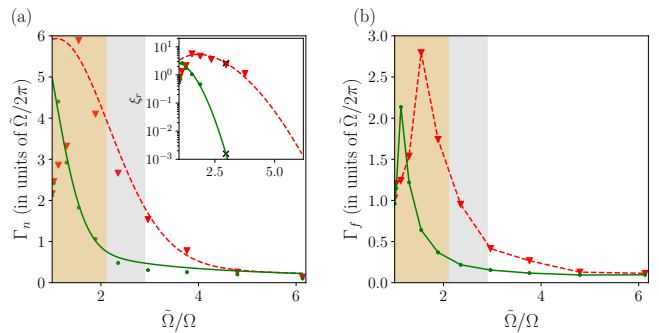


FIG. 4. Decay rates (a) Γ_n of average photon number and (b) Γ_f of fidelity for inhomogeneous width $\delta = 30$ MHz (red triangles) and $\delta = 60$ MHz (green dots), obtained from numerical calculations for $N = 100$ spins. The solid and dashed curves in (a) correspond to the theoretical value of $\zeta(\tilde{\Omega})$. The shaded region in both plots corresponds to the maximum squeezing of $r = 1.38$ (orange) achieved in experiment [43] and $r = 1.73$ (gray) in [45]. The inset in (a) shows the suppression in inhomogeneous broadening ξ_r calculated from Eq. (5), dot and triangle markers indicates the values computed from numerical simulations for $\delta = 30$ and 60 MHz, respectively. Black cross markers highlights the squeezing $r = 1.75$, where inhomogeneity is theoretically suppressed by a factor of 10^{-3} for $\delta = 30$ MHz.

encodes the information [50]. The decrease in $\mathcal{F}(t)$ corresponds to decoherence or loss of information, as the initially encoded state is no longer accurately accessible. This may take place due to inhomogeneous broadening, as well as other losses in the system. However, under increased parametric driving (higher values of r), the loss of fidelity is significantly minimized compared to the undriven system, thus highlighting a robust protection effect on the information encoded in the system. This is also evident in the phase-space properties of the information stored in the cavity as shown in Figs. 3(b)-(d), in terms of the Wigner function of $\rho_c(t)$. While Fig. 3(b), shows the $W(p, q)$ for the initially encoded state, Figs. 3(c) and (d) correspond to density matrices after one Rabi cycle for the undriven ($r = 0$) and the parametrically driven ($r = 2$) system, respectively. These plots clearly show that the phase coherence is better preserved for higher values of r .

Notably, for $r = 0$, the fidelity drops below 1/2 after one Rabi oscillation ($t \sim 1$), which is the probability of randomly guessing the stored information. However, under parametric driving, at large r the fidelity dies down at a rate governed by the losses in the system, while inhomogeneous broadening is suppressed. This highlights the strong protection experienced by the information stored in the hybrid quantum system.

Figure 4 shows the decay rates of average photon number and fidelity of information encoded in the initial state of the cavity. For $\delta = 30$ MHz, we see almost 10 fold reduction in both decay rates for $r = 1.5$ and this becomes 20 times at $r = 2.25$. Similar reduction in decay rates

id observed for $\delta = 60$ MHz as well. For $\tilde{\Omega} \gg \delta$, the theoretical decay rates match with the ones obtained numerically and cavity protection effect is visible for large squeezing r , with suppression in decay due to inhomogeneous broadening by a factor of 10^{-3} at $r = 1.75$ for inhomogeneous width of $\delta = 30$ MHz (see inset of Fig. 4(a)). In accordance with the mean-field calculations, irrespective of the width of the spectral distribution, the decay rate Γ_n approaches $\kappa + \gamma_h + 2\gamma_p$ in the limit of large r . However, the squeezing required to approach this limit increases as the width is increased, because countering high inhomogeneity requires stronger coupling with the cavity [15].

V. DISCUSSION

Hybrid quantum systems based on spin ensembles interacting with a cavity are ubiquitous in the design of quantum computing and communication architecture. As such, quantum information stored or transferred using these systems needs to be protected from decoherence arising due to inhomogeneity in the system. While there exist several sophisticated techniques to regain coherence, based on engineering of the spin distribution or using expensive cavities, the present results show that by simply using a parametric drive on the hybrid system and encoding information in the transformed states, an effective protection protocol can be achieved. It is to be noted that this protocol is significantly different from other applications of squeezed light such as its use for enhanced precision measurements [51, 52] or encoding information in continuous variable information processing [53–55].

From an experimental perspective, the use of higher-order interactions in hybrid systems can be naturally

adapted in the design of qubits, registers and quantum memories across a wide range of platforms, ranging from implementation of parametric driving in superconducting circuits [56, 57] and optomechanical devices [58] to the coupling of microwave resonators to ensembles based on electron spins [8], nitrogen-vacancy centers [9], and semiconductor qubits [59]. In recent studies, parametric modulation of potential has been used to observe enhanced effective interaction in trapped ions [41], while superradiant phase transition and strong entanglement has been observed in a nuclear magnetic resonance quantum simulator using antisqueezing effects [60].

Therefore, the protocol can be a powerful mechanism for designing versatile devices with significantly reduced error in information processing, and with much simpler engineering and low experimental overheads. Notably, the parametrically driven system can also be used to experimentally investigate regimes with ultrastrong coupling in ensembles, which will not only allow for the study of interesting protocols in quantum information but also throw more light on fundamental physics related to collective phenomena, many-body entanglement and nonequilibrium, driven-dissipative dynamics.

ACKNOWLEDGMENTS

We thank Sudipto Singha Roy for helpful suggestions and acknowledge the use of SpaceTime, the high-performance computing facility at IIT Bombay, for a part of the quantum simulations. H.S. acknowledges financial support from the Prime Minister’s Research Fellowship (ID: 1302055), Govt. of India. H.S.D. acknowledges funding from SERB-DST, India under Core-Research Grant (CRG/2021/008918) and IRCC, IIT Bombay (RD/0521-IRCCSH0-001).

-
- [1] K. Mølmer, Needle in a haystack, *Nature Phys.* **10**, 707 (2014).
 - [2] Z.-L. Xiang, S. Ashhab, J.Q. You, and F. Nori, Hybrid quantum circuits: Superconducting circuits interacting with other quantum systems, *Rev. Mod. Phys.* **85**, 623 (2013).
 - [3] G. Kurizki, P. Bertet, Y. Kubo, K. Mølmer, D. Petrosyan, P. Rabl, and J. Schmiedmayer, Quantum technologies with hybrid systems, *Proc. Natl. Acad. Sci. U.S.A.* **112**, 3866 (2015).
 - [4] Y. Nakamura, Yu. A. Pashkin, and J. S. Tsai, Coherent control of macroscopic quantum states in a single-Cooper-pair box, *Nature* **398**, 786 (1999).
 - [5] B. Julsgaard, J. Sherson, J.I. Cirac, J. Fiurášek, and E.S. Polzik, Experimental demonstration of quantum memory for light, *Nature* **432**, 482 (2004).
 - [6] C. Grezes, B. Julsgaard, Y. Kubo, M. Stern, T. Umeda, J. Isoya, H. Sumiya, H. Abe, S. Onoda, T. Ohshima, V. Jacques, J. Esteve, D. Vion, D. Esteve, K. Mølmer, and P. Bertet, Multimode storage and retrieval of microwave fields in a spin ensemble, *Phys. Rev. X* **4**, 021049 (2014).
 - [7] J. Verdú, H. Zoubi, Ch. Koller, J. Majer, H. Ritsch, and J. Schmiedmayer, Strong Magnetic Coupling of an Ultracold Gas to a Superconducting Waveguide Cavity, *Phys. Rev. Lett.* **103**, 043603 (2009).
 - [8] D.I. Schuster, A.P. Sears, E. Ginossar, L. DiCarlo, L. Frunzio, J.J.L. Morton, H. Wu, G.A.D. Briggs, B.B. Buckley, D.D. Awschalom, and R.J. Schoelkopf, High-Cooperativity Coupling of Electron-Spin Ensembles to Superconducting Cavities, *Phys. Rev. Lett.* **105**, 140501 (2010).
 - [9] Y. Kubo, F.R. Ong, P. Bertet, D. Vion, V. Jacques, D. Zheng, A. Dréau, J.-F. Roch, A. Auffeves, F. Jelezko, J. Wrachtrup, M.F. Barthe, P. Bergonzo, and D. Esteve, Strong Coupling of a Spin Ensemble to a Superconducting Resonator, *Phys. Rev. Lett.* **105**, 140502 (2010).
 - [10] R. Amsüss, Ch. Koller, T. Nöbauer, S. Putz, S. Rotter, K. Sandner, S. Schneider, M. Schramböck, G. Steinhäuser, H. Ritsch, J. Schmiedmayer, and J. Majer, Cavity QED with Magnetically Coupled Collective Spin States, *Phys. Rev. Lett.* **107**, 060502 (2011).
 - [11] J.H. Wesenberg, A. Ardavan, G.A.D. Briggs, J.J.L. Mor-

- ton, R.J. Schoelkopf, D.I. Schuster, and K. Mølmer, Quantum Computing with an Electron Spin Ensemble, *Phys. Rev. Lett.* **103**, 070502 (2009).
- [12] A.A. Clerk, K.W. Lehnert, P. Bertet, J.R. Petta, and Y. Nakamura, Hybrid quantum systems with circuit quantum electrodynamics, *Nature Phys.* **16**, 257 (2020).
- [13] A. Blais, A.L. Grimsmo, S.M. Girvin, and A. Wallraff, Circuit quantum electrodynamics, *Rev. Mod. Phys.* **93**, 025005 (2021).
- [14] Z. Kurucz, J.H. Wesenberg, and K. Mølmer, Spectroscopic properties of inhomogeneously broadened spin ensembles in a cavity, *Phys. Rev. A* **83**, 053852 (2011).
- [15] I. Diniz, S. Portolan, R. Ferreira, J. M. Gérard, P. Bertet, and A. Auffèves, Strongly coupling a cavity to inhomogeneous ensembles of emitters: Potential for long-lived solid-state quantum memories, *Phys. Rev. A* **84**, 063810 (2011).
- [16] S. Putz, D.O. Krimer, R. Amsüss, A. Valookaran, T. Nöbauer, J. Schmiedmayer, S. Rotter, and J. Majer, Protecting a spin ensemble against decoherence in the strong-coupling regime of cavity QED, *Nature Physics* **10**, 720 (2014).
- [17] D.O. Krimer, S. Putz, J. Majer, and S. Rotter, Non-Markovian dynamics of a single-mode cavity strongly coupled to an inhomogeneously broadened spin ensemble, *Phys. Rev. A* **90**, 043852 (2014).
- [18] B. Julsgaard, C. Grezes, P. Bertet, and K. Mølmer, Quantum Memory for Microwave Photons in an Inhomogeneously Broadened Spin Ensemble, *Phys. Rev. Lett.* **110**, 250503 (2013).
- [19] G. Bensky, D. Petrosyan, J. Majer, J. Schmiedmayer, and G. Kurizki, Optimizing inhomogeneous spin ensembles for quantum memory, *Phys. Rev. A* **86**, 012310 (2012).
- [20] J. Cai, F. Jelezko, N. Katz, A. Retzker, and M. B Plenio, Long-lived driven solid-state quantum memory, *New J. Phys.* **14**, 093030 (2012).
- [21] D.O. Krimer, B. Hartl, and S. Rotter, Hybrid Quantum Systems with Collectively Coupled Spin States: Suppression of Decoherence through Spectral Hole Burning, *Phys. Rev. Lett.* **115**, 033601 (2015).
- [22] S. Putz, A. Angerer, D.O. Krimer, R. Glattauer, W.J. Munro, S. Rotter, J. Schmiedmayer, and J. Majer, Spectral hole burning and its application in microwave photonics, *Nature Photon.* **11**, 36 (2017).
- [23] X.-Y. Lu, Y. Wu, J. R. Johansson, H. Jing, J. Zhang, and F. Nori, Squeezed Optomechanics with Phase-Matched Amplification and Dissipation, *Phys. Rev. Lett.* **114**, 093602 (2015).
- [24] S. Zeytinoglu, A. Imamoğlu, and S. Huber, Engineering Matter Interactions Using Squeezed Vacuum, *Phys. Rev. X* **7**, 021041 (2017).
- [25] W. Qin, A. Miranowicz, P.-B. Li, X.-Y. Lü, J.Q. You, and F. Nori, *Exponentially Enhanced Light-Matter Interaction, Cooperativities, and Steady-State Entanglement Using Parametric Amplification*, *Phys. Rev. Lett.* **120**, 093601 (2018).
- [26] C. Leroux, L.C.G. Govia, and A.A. Clerk, Enhancing cavity quantum electrodynamics via antisqueezing: Synthetic ultrastrong coupling, *Phys. Rev. Lett.* **120**, 093602 (2018).
- [27] Y. Wang, J.-L. Wu, J. Song, Z.-J. Zhang, Y.-Y. Jiang, and Y. Xia, *Enhancing atom-field interaction in the reduced multiphoton Tavis-Cummings model*, *Phys. Rev. A* **101**, 053826 (2020).
- [28] Y.H. Chen, W. Qin, X. Wang, A. Miranowicz, and F. Nori, Shortcuts to adiabaticity for the quantum rabi model: Efficient generation of giant entangled cat states via parametric amplification, *Phys. Rev. Lett.* **126**, 023602 (2021).
- [29] C.J. Zhu, L.L. Ping, Y.P. Yang, and G.S. Agarwal, *Squeezed Light Induced Symmetry Breaking Superradiant Phase Transition*, *Phys. Rev. Lett.* **124**, 073602 (2020).
- [30] S.-L. Yang, D.-Y. Lü, X.-K. Li, F. Badshah, L. Jin, Y.-H. Fu, G.-H. Wang, Y.-Z. Dong, Y. Zhou, *Manipulation of quantum phase transitions with Z2 symmetry for a realistic hybrid system*, *Results Phys.* **36**, 105425 (2022).
- [31] C.S. Muñoz and D. Jaksch, *Squeezed Lasing*, *Phys. Rev. Lett.* **127**, 183603 (2021).
- [32] R. Bonifacio and L. A. Lugiato, in *Dissipative Systems in Quantum Optics, Topics in Current Physics* (Springer-Verlag, Berlin, 1982).
- [33] D.O. Krimer, M. Zens, and S. Rotter, Critical phenomena and nonlinear dynamics in a spin ensemble strongly coupled to a cavity. I. Semiclassical approach, *Phys. Rev. A* **100**, 013855 (2019).
- [34] M. Zens, D.O. Krimer, and S. Rotter, Critical phenomena and nonlinear dynamics in a spin ensemble strongly coupled to a cavity. II. Semiclassical-to-quantum boundary, *Phys. Rev. A* **100**, 013856 (2019).
- [35] H.S. Dhar, M. Zens, D.O. Krimer, and S. Rotter, Variational Renormalization Group for Dissipative Spin-Cavity Systems: Periodic Pulses of Nonclassical Photons from Mesoscopic Spin Ensembles, *Phys. Rev. Lett.* **121**, 133601 (2018).
- [36] M. Tavis and F. W. Cummings, Exact solution for an N -molecule-radiation-field Hamiltonian, *Phys. Rev.* **170**, 379 (1968).
- [37] More generally, spin ensembles tend to have a q -Gaussian distribution [38] of width δ and a fixed value of $1 < q \leq 2$. For $q \rightarrow 1$, one obtains the Gaussian distribution, whereas $q = 2$ gives the Lorentzian distribution.
- [38] K. Sandner, H. Ritsch, R. Amsüss, Ch. Koller, T. Nöbauer, S. Putz, J. Schmiedmayer, and J. Majer, Strong magnetic coupling of an inhomogeneous nitrogen-vacancy ensemble to a cavity, *Phys. Rev. A* **85**, 053806 (2012).
- [39] C. Ciuti, G. Bastard, and I. Carusotto, Quantum vacuum properties of the intersubband cavity polariton field, *Phys. Rev. B* **72**, 115303 (2005).
- [40] A.F. Kockum, A. Miranowicz, S. De Liberato, S. Savasta, and F. Nori, Ultrastrong coupling between light and matter, *Nat. Rev. Phys.* **1**, 19 (2019).
- [41] S. C. Burd, R. Srinivas, H. M. Knaack, W. Ge, A. C. Wilson, D. J. Wineland, D. Leibfried, J. J. Bollinger, D. T. C. Allcock, and D. H. Slichter, Quantum amplification of boson-mediated interactions, *Nature Physics* **17**, 898 (2021).
- [42] M. Affolter, W. Ge, B. Bullock, S. C. Burd, K. A. Gilmore, J. F. Lillieholm, A. L. Carter, and J. J. Bollinger, Toward improved quantum simulations and sensing with trapped two-dimensional ion crystals via parametric amplification, *Phys. Rev. A* **107**, 032425 (2023).
- [43] S. C. Burd, H. M. Knaack, R. Srinivas, C. Arenz, A. L. Collopy, L. J. Stephenson, A. C. Wilson, D. J. Wineland, D. Leibfried, J. J. Bollinger, D. T. C. Allcock, and D. H. Slichter, Experimental speedup of quantum dynamics through squeezing, *PRX Quantum* **5**, 020314 (2024).
- [44] M. Villiers, W. C. Smith, A. Petrescu, A. Borgognoni, M. Delbecq, A. Sarlette, M. Mirrahimi, P. Campagne-

- Ibarcq, T. Kontos, and Z. Leghtas, Dynamically enhancing qubit-photon interactions with antisqueezing, *PRX Quantum* **5**, 020306 (2024).
- [45] H. Vahlbruch, M. Mehmet, K. Danzmann, and R. Schnabel, Detection of 15 db squeezed states of light and their application for the absolute calibration of photoelectric quantum efficiency, *Phys. Rev. Lett.* **117**, 110801 (2016).
- [46] U. Schollwoeck, The density-matrix renormalization group in the age of matrix product states, *Ann. Phys.* **326**, 96 (2011).
- [47] M. Zens, H.S. Dhar, D.O. Krimer, and S. Rotter, Periodic Cavity State Revivals from Atomic Frequency Combs, *Phys. Rev. Lett.* **127**, 180402 (2021).
- [48] A.J. Daley, C. Kollath, U. Schollwöck, and G. Vidal, Time-dependent density-matrix renormalization-group using adaptive effective Hilbert spaces, *J. Stat. Mech.* **P04005** (2004).
- [49] S.R. White and A.E. Feiguin, Real-Time Evolution Using the Density Matrix Renormalization Group, *Phys. Rev. Lett.* **93**, 076401 (2004).
- [50] The envelope is taken for representation as the cavity state regains all its coherence only at specific times. The actual fidelity oscillates as information is coherently exchanged between the spin ensemble and the cavity modes.
- [51] M. Xiao, L.-A. Wu, and H.J. Kimble, Precision measurement beyond the shot-noise limit, *Phys. Rev. Lett.* **59**, 278 (1987).
- [52] R. Schnabel, Squeezed states of light and their applications in laser interferometers, *Phys. Rep.* **684**, 1 (2017).
- [53] S.L. Braunstein and P. van Loock, Quantum information with continuous variables, *Rev. Mod. Phys.* **77**, 513 (2005).
- [54] S. Takeda, T. Mizuta, M. Fuwa, P. van Loock, and A. Furusawa, Deterministic quantum teleportation of photonic quantum bits by a hybrid technique, *Nature* **500**, 315 (2013).
- [55] K. Park, J. Hastrup, J.S. Neergaard-Nielsen, J.B. Brask, R. Filip, and U.L. Andersen, Slowing quantum decoherence of oscillators by hybrid processing, *npj Quantum Inf.* **8**, 67 (2022).
- [56] B. Royer, S. Puri, and A. Blais, Qubit parity measurement by parametric driving in circuit QED, *Science Advances* **4**, eaau1695, (2018).
- [57] A. Eddins, J.M. Kreikebaum, D.M. Toyli, E.M. Levenson-Falk, A. Dove, W.P. Livingston, B.A. Levitan, L.C.G. Govia, A.A. Clerk, and I. Siddiqi, High-Efficiency Measurement of an Artificial Atom Embedded in a Parametric Amplifier, *Phys. Rev. X* **9**, 011004 (2019).
- [58] M. Aspelmeyer, T.J. Kippenberg, and F. Marquardt, Cavity optomechanics, *Rev. Mod. Phys.* **86**, 1391 (2014).
- [59] X. Mi, J.V. Cady, D.M. Zajac, P.W. Deelman, and J.R. Petta, Strong coupling of a single electron in silicon to a microwave photon, *Science* **355**, 156 (2017).
- [60] X. Chen, Z. Wu, M. Jiang, X.-Y. Lü, X. Peng, and J. Du, Experimental quantum simulation of superradiant phase transition beyond no-go theorem via antisqueezing, *Nature Commun.* **12**, 6281 (2021).